

The UAP56-Interacting Export Factors UIEF1 and UIEF2 Function in mRNA Export¹[OPEN]

Hans F. Ehrnsberger,^a Christina Pfaff,^a Ines Hachani,^a María Flores-Tornero,^a Brian B. Sørensen,^a Gernot Längst,^b Stefanie Sprunck,^a Marion Grasser,^{a,2} and Klaus D. Grasser^{a,3}

^aDepartment of Cell Biology & Plant Biochemistry, Biochemistry Centre, University of Regensburg, D-93053 Regensburg, Germany

^bDepartment of Biochemistry III, Biochemistry Centre, University of Regensburg, D-93053 Regensburg, Germany

ORCID IDs: 0000-0002-0007-0485 (H.F.E.); 0000-0002-8232-1179 (G.L.); 0000-0002-9732-9237 (S.S.); 0000-0002-7618-1974 (M.G.); 0000-0002-7080-5520 (K.D.G.).

In eukaryotes, the regulated transport of mRNAs from the nucleus to the cytosol through nuclear pore complexes represents an important step in the expression of protein-coding genes. In plants, the mechanism of nucleocytoplasmic mRNA transport and the factors involved are poorly understood. The *Arabidopsis thaliana* genome encodes two likely orthologs of UAP56-interacting factor, which acts as mRNA export factor in mammalian cells. In yeast and plant cells, both proteins interact directly with the mRNA export-related RNA helicase UAP56 and the interaction was mediated by an N-terminal UAP56-binding motif. Accordingly, the two proteins were termed UAP56-INTERACTING EXPORT FACTOR1 and 2 (UIEF1/2). Despite lacking a known RNA-binding motif, recombinant UIEF1 interacted with RNA, and the C-terminal part of UIEF1 mainly contributed to the RNA interaction. Mutation of *UIEF1*, *UIEF2*, or both in the double-mutant *2xuief* caused modest growth defects. A cross between the *2xuief* and *4xaly* (defective in the four ALY1–4 mRNA export factors) mutants produced the sextuple mutant *4xaly 2xuief*, which displayed more severe growth impairment than the *4xaly* plants. Developmental defects including delayed bolting and reduced seed set were observed in the *4xaly* but not the *2xuief* plants. Analysis of the cellular distribution of polyadenylated mRNAs revealed more pronounced nuclear mRNA accumulation in *4xaly 2xuief* than in *2xuief* and *4xaly* cells. In conclusion, the results indicate that UIEF1 and UIEF2 act as mRNA export factors in plants and that they cooperate with ALY1–ALY4 to mediate efficient nucleocytoplasmic mRNA transport.

Subsequent to synthesis and complete processing, mature mRNAs are exported from the nucleus to the cytosol for translation. Ongoing work has identified a multitude of proteins that facilitate the transport of export-competent mRNAs across the nuclear envelope through nuclear pore complexes (NPCs; Köhler and Hurt, 2007; Wickramasinghe and Laskey, 2015). Because many of these export factors are recruited cotranscriptionally to the pre-mRNAs, the nucleocytoplasmic transport of mRNAs is an integral step in

mRNP biogenesis. The TRanscription-EXport (TREX) complex was identified as a pivotal player connecting transcription, processing, and export (Katahira, 2012; Heath et al., 2016). TREX is composed of the suppressors of the transcriptional defects of *hpr1Δ* by an overexpression (THO) core complex that interacts with additional proteins such as the RNA helicase UAP56 (Sub2 in yeast) and mRNA export factors such as Tho1 in yeast (CIP29) and Yra1 in yeast (ALY; Strässer et al., 2002; Masuda et al., 2005; Dufu et al., 2010). In metazoa, TREX is recruited cotranscriptionally to mRNAs in a capping-, splicing-, and polyadenylation-dependent manner (Katahira, 2012; Heath et al., 2016). UAP56 performs a critical function initiating the nucleocytoplasmic transport of mRNAs by loading various types of mRNA export adaptors such as ALY onto both spliced and intronless mRNAs (Luo et al., 2001; Taniguchi and Ohno, 2008). Thus, mRNA adaptors are recruited to the nascent mRNA during transcriptional elongation dependent on processing events, finally licensing correctly synthesized and completely processed mRNAs for export (Walsh et al., 2010). Subsequently, the export adaptors in combination with other TREX components load the mRNA export receptor NXF1/NXT1 (Mex67/Mtr2 in yeast) onto the mRNA (Viphakone et al., 2012). Ultimately,

¹This work was supported by the German Research Foundation (DFG grant SFB960 to K.D.G.).

²Senior author.

³Author for contact: klaus.grasser@ur.de.

The author responsible for distribution of materials integral to the findings presented in this article in accordance with the policy described in the Instructions for Authors (www.plantphysiol.org) is: Klaus Grasser (klaus.grasser@ur.de).

M.G. and K.D.G. conceived the project; G.L., S.S., M.G., and K.D.G. supervised the project; H.F.E., C.P., I.H., M.F.-T., B.B.S., and M.G. conducted experiments; H.F.E., C.P., I.H., M.F.-T., B.B.S., G.L., S.S., M.G., and K.D.G. analyzed the data; S.S., M.G., and K.D.G. wrote the article; all authors read and approved the final manuscript.

[OPEN]Article can be viewed without a subscription.

www.plantphysiol.org/cgi/doi/10.1104/pp.18.01476

NXF1/NXT1 interacts with TREX-2 at the NPC and Phe/Gly repeats of nucleoporins, facilitating translocation of the mRNA to the cytosolic side of the NPC (Katahira, 2012; Wickramasinghe and Laskey, 2015; Heath et al., 2016).

Currently, comparatively little is known about the mRNA export pathway in plants (Xu and Meier, 2008; Merkle, 2011; Gaouar and Germain, 2013). Proteomics approaches demonstrated that the THO core complex of TREX in *Arabidopsis* (*Arabidopsis thaliana*) shares the composition of metazoan THO rather than that of yeast (Yelina et al., 2010), and, based on in situ hybridization analyses using oligo(dT) probes, THO subunits are required for efficient mRNA export (Pan et al., 2012; Xu et al., 2015; Sørensen et al., 2017). More recently, it was shown that THO interacts with the ATP-dependent DEAD-box RNA helicase UAP56 (Sørensen et al., 2017). Mediated by direct interactions with UAP56, MOS11 (the ortholog of CIP29) and four different ALY proteins are also part of *Arabidopsis* TREX (Kammell et al., 2013; Sørensen et al., 2017; Pfaff et al., 2018). To date, only the UAP56-associated plant proteins, namely MOS11 and ALY1–4, were experimentally shown to be involved in plant mRNA export, as *mos11* and *4xaly* mutants exhibit nuclear mRNA accumulation (Germain et al., 2010; Pfaff et al., 2018). The ALY export adaptor proteins are diversified in plants, and the *Arabidopsis* genome encodes four family members termed ALY1–4. Single- and double-mutant plants have largely a wild-type appearance, whereas the quadruple mutant termed *4xaly* (deficient in all ALY1–4 proteins) displays various vegetative and reproductive defects (Pfaff et al., 2018).

Inactivation of yeast Yra1 (the ortholog of ALY) leads to a severe mRNA export block and cells lacking Yra1 are not viable (Strässer and Hurt, 2000; Zenklusen et al., 2001). In mammals, *Drosophila melanogaster* and *Caenorhabditis elegans* knock-down of ALY genes has no significant impact on global mRNA export (Gatfield and Izaurralde, 2002; Longman et al., 2003; Katahira et al., 2009). Similarly, individual *Arabidopsis* *aly1–4* mutants show no mRNA export defect, but simultaneous inactivation of the four ALY1–4 genes in the *4xaly* mutant results in a partial mRNA export block (Pfaff et al., 2018). These findings suggest the existence of additional mRNA export adaptors with possible (partial) functional redundancy (Walsh et al., 2010). Actually, in mammals, several proteins were identified that contain a conserved UAP56-binding motif (UBM) and, accordingly, via UAP56 interactions, are components of TREX. These proteins comprise UAP56-interacting factor (UIF), Chtop, and Luzp4 (which have no orthologs in yeast), and they can act as mRNA export adaptors similar to ALY (Hautbergue et al., 2009; Chang et al., 2013; Viphakone et al., 2015).

In light of the partial mRNA export block of the *Arabidopsis* *4xaly* mutant and the existence of further mammalian mRNA export adaptors in addition to ALY, we analyzed whether the *Arabidopsis* genome encodes other mRNA export adaptor candidates. Our

bioinformatics survey revealed no sequences related to Chtop and Luzp4, but two proteins with similarity to human UIF that, to date, had not been experimentally analyzed. Therefore, we examined the encoded proteins as well as corresponding mutant plants. The UIF-like RNA-binding proteins interact with UAP56 and plants lacking these two proteins are phenotypically mildly affected and they display modest nuclear mRNA accumulation. Both the phenotypic effects and the reduced mRNA export are additive with the defects of *4xaly* plants. These findings identify the two UIF-like proteins as plant mRNA export factors.

RESULTS

Plant Genomes Encode Proteins with Similarity to the Human mRNA Export Factor UIF

We used the amino acid sequences of human UIF, Chtop, and Luzp4 to search the *Arabidopsis* database (<https://www.arabidopsis.org/>) using BLAST for similar sequences. The search did not yield sequences related to Chtop and Luzp4, but consistent with the original report on human UIF (Hautbergue et al., 2009), two *Arabidopsis* genes were found to encode UIF-like proteins that to date have not been experimentally validated. Because the term “UIF” is used in *Arabidopsis* for an unrelated protein, we designated the two proteins “UAP56-INTERACTING EXPORT FACTOR1/2” (UIEF1/2). The predicted amino acid sequences of UIEF1 and UIEF2 are 48.4% identical and both UIEF1 (24.5 kD) and UIEF2 (22.3 kD) are basic proteins (pI ~ 11.7) rich in Arg and Lys residues. They share ~18% amino acid sequence identity with human UIF (35.8 kD), and thus are only moderately related to their mammalian orthologs.

Further database searches using the UIEF1/2 sequences demonstrated that closely related proteins are encoded in monocot and dicot plants. As with *Arabidopsis*, two genes each were detected in soybean (*Glycine max*), poplar (*Populus trichocarpa*), and maize (*Zea mays*), whereas in rice (*Oryza sativa*) and *Sorghum bicolor*, UIEF seems to be encoded by single-copy genes. Aligning these sequences showed that the region around the putative N-terminal UBM is the most highly conserved part of these proteins (Supplemental Fig. S1). Apart from the putative UBM, no discernible protein domains were recognized in the UIEF1/2 amino acid sequences. More distantly related sequences were identified in *Selaginella*, *Physcomitrella*, and *Amborella* (Supplemental Fig. S2). In addition to mammals and plants, UIF-like sequences were identified in certain animals, but apparently closely related proteins do not exist in all animal species (Hautbergue et al., 2009).

UIEF1/2 Interact Directly with UAP56

A key feature of ALY-/UIF-related mRNA export factors is their interaction with the RNA helicase

UAP56 linking them to the TREX complex (Walsh et al., 2010). Therefore, we examined whether UIEF1/2 interact with UAP56 in a yeast two-hybrid assay. In Arabidopsis, an identical UAP56 protein is encoded by two adjacent genes (Kammel et al., 2013), and we used the sequence of *UAP56a* (At5g11170) for the experiments described here. UIEF1/2 and UAP56 fused to the Gal4 activation domain (AD) or the DNA-binding domain (BD) were expressed in yeast cells. Yeast cells coexpressing both types of fusion proteins (AD + BD) were scored for growth on double dropout (DDO) and the high-stringency, selective quadruple dropout (QDO) media. All strains grew on DDO medium, demonstrating successful transformation (Fig. 1B). On QDO medium, combinations of UAP56 and UIEF1/2 (along with a positive control) were able to grow, whereas cells expressing a negative control showed no growth. To test whether the putative UBM of UIEF1 (Fig. 1A) mediates the interaction with UAP56, three conserved amino acid residues of the motif were mutated to create UIEF1m. Cells coexpressing UIEF1m-AD and UAP56-BD formed colonies on DDO medium, but were unable to grow on QDO medium (Fig. 1B), revealing that mutating the UBM of UIEF1 abolished the interaction with UAP56. These experiments demonstrate that UIEF1/2 interact with UAP56 in yeast cells.

Additionally, the interaction between UIEF1/2 and UAP56 was examined using Förster resonance energy transfer (FRET). eGFP and mCherry fusion proteins acting as donor/acceptor pairs were expressed in *Nicotiana benthamiana* leaves. The recovery of donor fluorescence after acceptor photobleaching (APB) was quantified. Cells expressing UIEF1/2 fused to eGFP along with unfused mCherry provided background levels (FRET-APB efficiencies $0.7 \pm 1.4\%$ and $0.3 \pm 1.1\%$, respectively) of the experiment, whereas an eGFP-mCherry fusion protein (FRET-APB efficiency $23.7 \pm 4.8\%$) served as a positive control (Fig. 1C). For the combinations UIEF1-eGFP with UAP56-mCherry and UIEF2-eGFP with UAP56-mCherry, FRET-APB efficiencies of $8.5 \pm 1.5\%$ and $8.2 \pm 2.5\%$, respectively, were recorded. For the UBM-mutated version UIEF1m-eGFP in combination with UAP56-mCherry, only background levels were measured. Thus, UIEF1 and UIEF2 interact directly with UAP56 both in yeast and *N. benthamiana* cells, and in the case of UIEF1, the interaction is mediated by the UBM.

UIEF1 Interacts with RNA

As putative mRNA export factors, UIEF1/2 are predicted to have RNA-binding activity. However, UIEF1/2 do not contain recognizable RNA-binding motifs like their human ortholog UIF, which nevertheless was found to bind RNA (Hautbergue et al., 2009). We selected UIEF1 to study its RNA interactions. In addition to full-length UIEF1 (M1-N217), the N-terminal part (M1-S101, termed "UIEF1 Δ C") and the C-terminal part (A102-N217, termed "UIEF1 Δ N") were

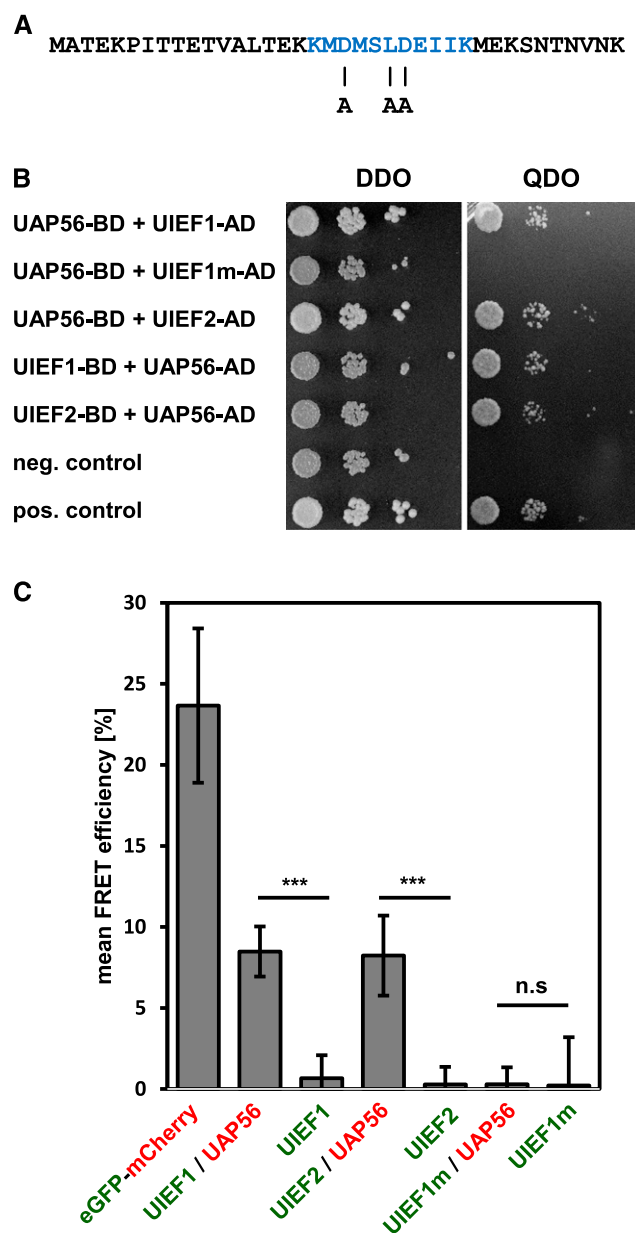


Figure 1. UIEF1/2 interact with UAP56 in yeast and plant cells. **A**, N-terminal amino acid sequence of UIEF1. The UBM is highlighted and the residues that were changed into Ala residues in UIEF1m are indicated by (A). **B**, Yeast two-hybrid assays with cells harboring the indicated constructs grown on DDO (left) or QDO (right) media. **C**, Protein interactions analyzed by acceptor-photobleaching FRET. *N. benthamiana* leaves were coinfiltrated with vectors (x axis) directing the expression of the indicated donor (eGFP, green)-acceptor (mCherry, red) combinations as well as of positive and negative controls. Transiently transformed cells were analyzed in two biological replicates by FRET-APB. Mean FRET-APB efficiencies (\pm SD, eight analyzed nuclei each) are shown, which were analyzed using Student's *t* test (***) $P < 0.001$; n.s.: nonsignificant).

expressed in *Escherichia coli* as 6xHis-GB1 fusion proteins. The three recombinant proteins were purified by two-step chromatography and analyzed by sodium

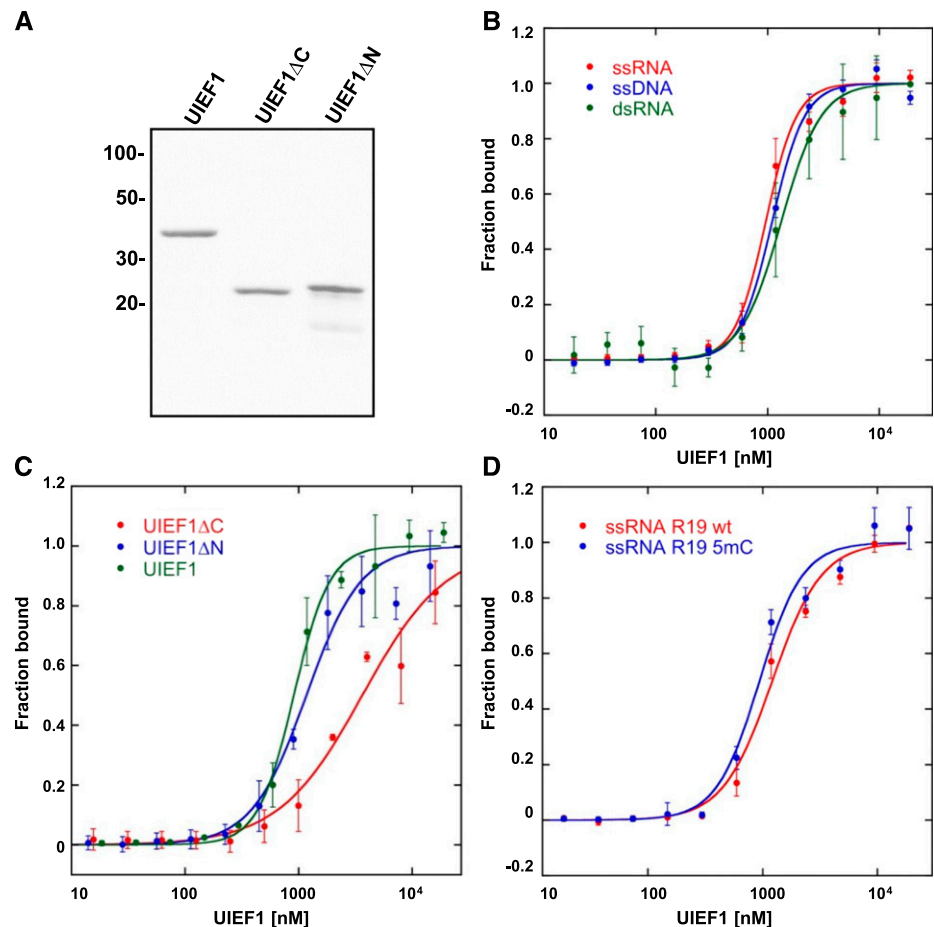
dodecyl sulfate-polyacrylamide gel electrophoresis (SDS-PAGE; Fig. 2A). The recombinant proteins were examined for RNA-binding in solution using Micro-Scale Thermophoresis (MST). As demonstrated before (Pfaff et al., 2018), the unfused 6xHis-GB1 tag does not interact with RNA (Supplemental Fig. S3). Full-length UIEF1 bound ssRNA ($EC_{50} = 964 \pm 39$ nM) with marginally higher affinity than ssDNA and dsRNA ($EC_{50} = 1,099 \pm 35$ nM and $1,325 \pm 78$ nM, respectively; Fig. 2B). Comparative analysis of the RNA-binding of full-length and the two truncated UIEF1 proteins (Fig. 2C) revealed that UIEF1 Δ N ($EC_{50} = 1,099 \pm 35$ nM) interacted with the ssRNA almost as efficiently as UIEF1 ($EC_{50} = 907 \pm 43$ nM). In contrast, UIEF1 Δ C ($EC_{50} = 3,632 \pm 791$ nM) bound with ~ 4 -fold lower affinity to the ssRNA probe, suggesting that the C-terminal part of the protein primarily mediates the RNA interactions. Because human ALY (Yang et al., 2017) and Arabidopsis ALY1 (Pfaff et al., 2018) preferentially interact with 5-methylcytosine (m^5C)–modified RNA, we tested whether UIEF1 shares this feature (Fig. 2D). However, UIEF1 bound the m^5C -modified probe with only marginally higher affinity ($EC_{50} = 936 \pm 78$ nM) than that of the unmodified RNA ($EC_{50} = 1,208 \pm 94$ nM), indicating that UIEF1 displays no clear preference for m^5C -modified RNA.

Expression and Subcellular Localization of the UIEF1/2 Proteins

To analyze the expression and subcellular localization of UIEF1/2-GFP fusion proteins in the absence of the respective endogenous protein, we characterized T-DNA insertion lines disrupted in the *UIEF1/2* genes. Based on genotyping and sequencing of the corresponding genomic regions, plants homozygous for T-DNA insertions within exon 2 of *UIEF1* and within exon 3 of *UIEF2* were obtained (Supplemental Fig. S4, A and B). Analysis of the transcript levels by reverse transcription (RT)-PCR demonstrated that the respective *UIEF1/2* transcript was not detectable in the mutant plants and that the level of the other *UIEF1/2* transcript was comparable to that observed in the wild-type Col-0 (Supplemental Fig. S4C). The two *uief1/2* mutant lines are phenotypically only mildly affected, and were transformed with the respective UIEF1/2-GFP fusion constructs under control of the native promoters. Different UIEF1/2-GFP expression lines were examined by RT-PCR for the expression of *UIEF1/2* relative to that in Col-0. These analyses showed that the *UIEF1/2* transcript levels in the complemented lines are comparable to those in Col-0 (Supplemental Fig. S5).

After staining with propidium iodide, primary root tips of the plants expressing UIEF1/2-GFP fusion

Figure 2. Production of recombinant UIEF1 proteins and MST analysis of their interaction with nucleic acids. A, Full-length UIEF1 and truncated versions of the protein (fused to a 6xHis-GB1 tag) were expressed in *E. coli*, purified, and the SDS-PAGE analysis of the purified proteins after Coomassie staining is shown. Numbers on the left indicate the migration position of molecular weight markers. B, MST analysis of the interaction of full-length UIEF1 with different types of 25-nt nucleic acid probes. C, MST analysis of the interaction of full-length and truncated versions of UIEF1 with 25-nt ssRNA. D, MST analysis of the interaction of full-length UIEF1 with m^5C -modified 19-nt ssRNA and with the unmodified control RNA. Measurements were performed with each two biological and two technical replicates, and error bars indicate sd of the biological replicates.



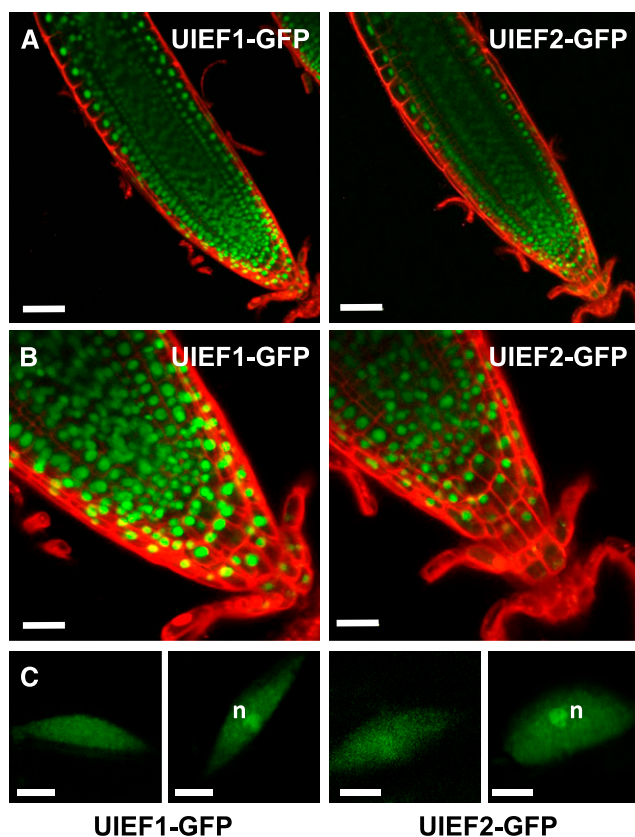


Figure 3. UIEF1/2 GFP-fusion proteins as visualized by CLSM in nuclei of root cells. A, Root tips of 8-DAS plants expressing the indicated GFP fusion proteins under control of the respective native promoters. GFP fluorescence is visible in green, whereas propidium iodide staining is in red. B, Root tips shown at higher magnification. C, Subnuclear localization of UIEF1/2. Examples of root cell nuclei are shown, illustrating the variable distribution of UIEF1-GFP (first and second left) and UIEF2-GFP (third and fourth right). In cells with nucleolar enrichment of UIEF1/2, nucleoli are indicated by *n*. Size bars = 50 μm (A), 20 μm (B), and 5 μm (C).

proteins were analyzed by confocal laser scanning microscopy (CLSM). Both UIEF1/2 proteins were detected exclusively in the nuclei of all root cells (Fig. 3, A and B). Similar to the situation with the ALY1–4 proteins (Pfaff et al., 2018), we also detected UIEF1/2 to various extents in nucleoli (Fig. 3C). In some cells, UIEF1 and UIEF2 similarly display nucleolar accumulation relative to nucleoplasmic localization ($60 \pm 7\%$ and $64 \pm 2\%$, respectively, each 90 nuclei analyzed from three independent roots). We also noted that, compared to the ALY-GFP fusion proteins (Pfaff et al., 2018), the GFP fluorescence was much weaker, indicating considerably lower expression levels of both the UIEF1- and UIEF2-GFP fusion proteins. The lower expression of UIEF1/2-GFP relative to that of ALY1/3-GFP is illustrated by CLSM images taken at the same time with identical microscope settings (Supplemental Fig. S6). Due to the lower expression, we were unable to detect unambiguous UIEF1/2-GFP signals in leaf cells, although consistent with public transcript profiling data

(Supplemental Fig. S7), UIEF1/2 transcripts are detectable by RT-PCR in the aerial part of the plants (Supplemental Figs. S4 and S5).

uief1 and *uief2* Mutant Plants Are Mildly Affected in Growth and Nuclear mRNA Accumulation

The absence of UIEF1/2 in the homozygous *uief1* and *uief2* mutant plants had only slight impact on the phenotype. Accordingly, *uief1 uief2* double-mutants (herein termed “*2xuief*”) were generated that also displayed subtle differences when compared to the Col-0 phenotype. The single- and double-mutants were moderately smaller than Col-0, as evident from the reduced rosette diameter and plant height (Fig. 4; Supplemental Fig. S8). The *2xuief* plants were hardly more affected than the single-mutant plants. Regarding bolting time, number of leaves at bolting, and growth of the primary root, no difference relative to that of Col-0 was observed (Fig. 4; Supplemental Fig. S8).

To examine whether the plants deficient in UIEF1/2 are affected in nucleocytoplasmic mRNA distribution, in situ hybridization of seedling root tips with a fluorescently labeled oligo(dT) probe (Gong et al., 2005) was performed to detect bulk poly(A) mRNA. Relative to the cytosolic signals, stronger fluorescence was detected similarly in the nuclei of the *uief1* and *uief2* single and the *2xuief* double mutants when compared with that of Col-0 (Supplemental Fig. S9). The increased nuclear retention of polyadenylated mRNAs in *2xuief* plants observed in situ hybridization analyses is consistent with a role of UIEF1/2 in mRNA export.

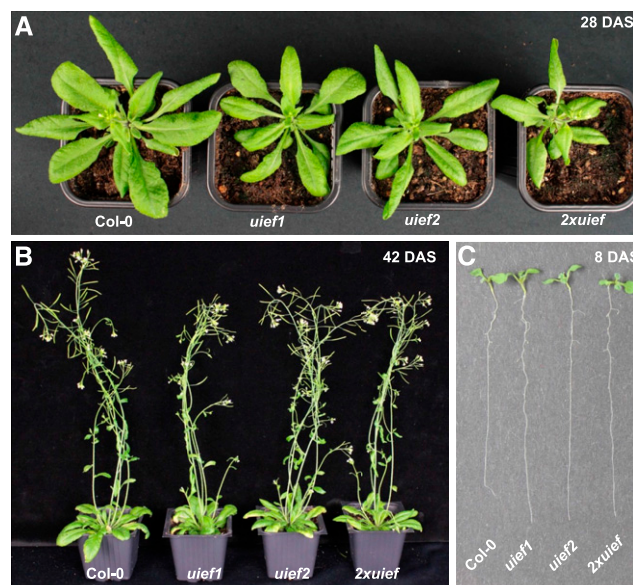


Figure 4. Phenotype of *uief1* and *uief2* single- and double-mutant (*2xuief*) plants relative to that of Col-0. A and B, Representative images of plants at 28 DAS (A) and 42 DAS (B) grown under LD conditions in soil. C, Roots of 8-DAS seedlings grown on solid MS medium.

The *uief1* and *uief2* Mutations Reduce the Rosette Growth of *4xaly* Plants, But They Do Not Reinforce the Reproductive Defects

In view of the relatively weak effects caused by the *uief1* and *uief2* mutations, we generated mutant plants affected in expression of the *UIEF1/2* genes (*2xuief*) as well as in the expression of the *ALY1–4* genes (*4xaly*) resulting in the corresponding sextuple mutant *4xaly 2xuief*. Plants homozygous for the mutations in the *UIEF1/2* and *ALY1–4* genes are viable, but they are more severely impacted regarding some morphological phenotypes than that observed in the previously characterized *4xaly* plants (Pfaff et al., 2018). Compared to that in *4xaly*, the rosette diameter is reduced in *4xaly 2xuief* plants, whereas *4xaly* and *4xaly 2xuief* plants are comparable regarding bolting time, number of leaves at bolting, plant height, and growth of the primary root (Fig. 5; Supplemental Fig. S10). Hence, the *uief1* and *uief2* mutations enhance the growth defects of the rosette leaves observed in *4xaly* plants.

Recently, we have shown that *4xaly* plants exhibit altered flower morphologies with incomplete penetrance. Approximately 25% of the *4xaly* flowers revealed phenotypes including altered number of petals (ranging from 3 to 7), markedly increased number of trichomes on the sepals, or severely reduced length of the stamen filaments. We furthermore observed female reproductive defects in the *4xaly* mutant caused by abnormal development of ovule integuments and female gametophytes, respectively, whereas male gametophyte development and function was

apparently unaffected (Pfaff et al., 2018). Compared with that in Col-0, neither flower morphology nor ovule development were significantly changed in the *2xuief* mutant (Supplemental Fig. S11). Furthermore, the seed set in siliques of *2xuief* plants was comparable to that of wild-type siliques (Fig. 6).

As the reproductive phenotypes in *4xaly* showed incomplete penetrance, we investigated whether the altered flower and ovule morphologies are potentiated in the *4xaly 2xuief* mutant. However, neither the percentage of individuals with altered flower morphologies, mutant ovule, nor female gametophyte phenotypes were significantly increased in the *4xaly 2xuief* genotype (Supplemental Fig. S11, A–K). In vitro pollen germination rates for *4xaly 2xuief* were comparable to those obtained for *2xuief*, *4xaly*, and Col-0 (Supplemental Fig. S11, L–O). The observation that *4xaly* and *4xaly 2xuief* mutant plants showed similar reduced seed set (Fig. 6) indicated that no additive reproductive phenotypes arise when *UIEF1* and *UIEF2* are lacking in the *4xaly* background.

The Lack of *UIEF1/2* Enhances the Nuclear mRNA Accumulation of *4xaly* Plants

To assess whether the *uief1/2* mutations add to the mRNA export defect of *4xaly* plants, *2xuief*, *4xaly*, and *4xaly 2xuief*, along with Col-0 plants, were examined using in situ hybridization with a fluorescently labeled oligo(dT) probe and CLSM. All mutant lines showed (relative to the cytosolic signal) a stronger nuclear fluorescence signal than that in Col-0 (Fig. 7). A relative potentiation of the nuclear accumulation of polyadenylated mRNAs was observed in the different genotypes in the following order: Col-0 < *2xuief* < *4xaly* < *4xaly 2xuief*. Therefore, the in situ hybridization experiments revealed an increased nuclear mRNA retention of *2xuief* and *4xaly* plants, when compared to that of Col-0. Moreover, the simultaneous loss of *UIEF1/2* and *ALY1–4* proteins in the *4xaly 2xuief* plants caused additive effects on the nucleocytoplasmic transport of mRNAs, indicating that *UIEF1/2* and *ALY1–4* proteins are jointly involved in the mRNA export from plant nuclei.

Because the *UIEF1/2* (and *ALY1–4*) proteins occur to some extent in nucleoli in addition to the nucleoplasm, we analyzed whether they influence rRNA abundance. We employed a Bioanalyser based on microfluidic electrophoresis for sizing and quantifying rRNA species of total RNA samples. The ratios of cytosolic and plastid rRNA species of the large and small ribosomal subunits were measured as a proxy for the accumulation of rRNAs (Walter et al., 2010; Fleischmann et al., 2011). The *2xuief*, *4xaly*, and *4xaly 2xuief* mutant lines were analyzed comparatively with Col-0. These measurements revealed that the 18S rRNA: 16S rRNA and the 26S rRNA: 16S rRNA ratios are comparable in the analyzed mutant plants and Col-0 (Supplemental Fig. S12), consistent with an unchanged cytosolic rRNA

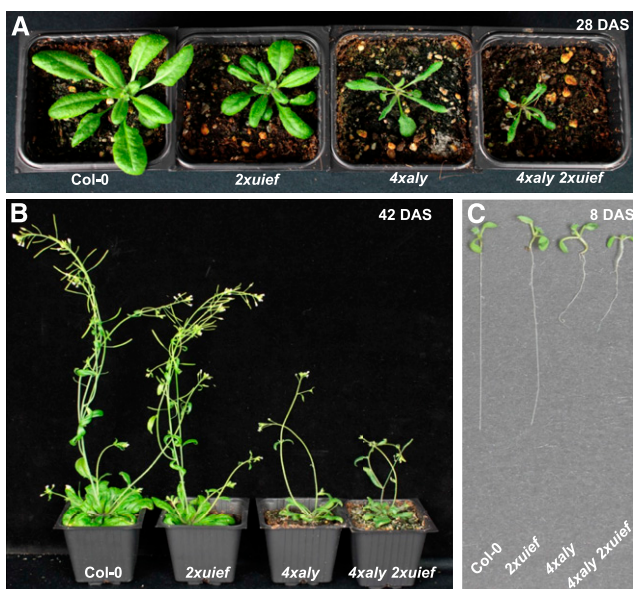


Figure 5. Phenotype of *2xuief* and *4xaly* mutant plants relative to that of the sextuple mutant *4xaly 2xuief* (defective in the *ALY1–4* and *UIEF1/2* genes) and Col-0. A and B, Representative images of plants at 28 DAS (A) and 42 DAS (B) grown under LD conditions in soil. C, Roots of 8-DAS seedlings grown on solid MS medium.

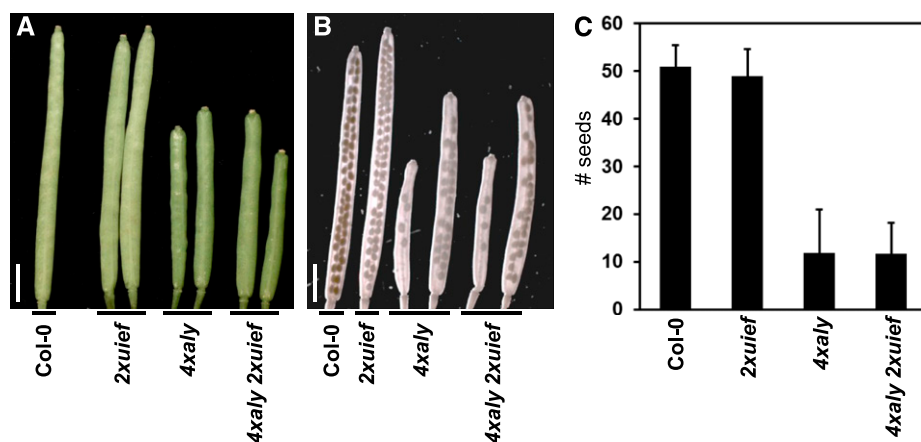


Figure 6. Seed set of *2xuiief*, *4xaly*, and *4xaly 2xuiief* mutants in comparison to that of Col-0. A, Comparison of silique length. *4xaly* and *4xaly 2xuiief* mutant siliques are shorter than those of Col-0 and *2xuiief*. B, Comparison of silique seed content using cleared siliques. *4xaly* and *4xaly 2xuiief* mutant siliques contain fewer seeds. C, Quantification of the number of seeds per silique in *2xuiief*, *4xaly*, *4xaly 2xuiief*, and Col-0 (x axis). Results show the mean, and bars represent the SD ($n = 35$ siliques per genotype). Scale bars = 2 mm (A and B).

accumulation in the mutant plants. This suggests that in Arabidopsis, as in yeast and metazoa (Peña et al., 2017), rRNA is exported by mechanisms independent of proteins like ALY and UIF.

DISCUSSION

Research performed in yeast and metazoa has established that tRNAs, miRNAs, snRNAs, and rRNAs are exported from the nucleus by mechanisms that involve exportins of the karyopherin class and the Ran cycle. In contrast, nucleocytoplasmic transport of bulk mRNAs generally is mechanistically different and not directly dependent on Ran GTPase activity (Köhler and Hurt, 2007; Williams et al., 2018). Numerous export factors including the THO complex, UAP56, and

various mRNA export adaptors such as ALY/UIF and the NXF1/NXT1 export receptor, cooperate to mediate translocation of mRNAs through NPCs (Wickramasinghe and Laskey, 2015; Heath et al., 2016). This process that links nuclear mRNA synthesis with cytosolic translation ensures that only properly synthesized and processed transcripts are exported (Wickramasinghe and Laskey, 2015; Heath et al., 2016). The mechanism and the involved components of mRNA export are poorly characterized in plants (Xu and Meier, 2008; Merkle, 2011; Gaouar and Germain, 2013). We have studied here the Arabidopsis UIF1/2 proteins that are structurally related to the human UIF mRNA export adaptor (Hautbergue et al., 2009). Both UIF1 and UIF2 interacted with the DEAD-box RNA helicase UAP56 in yeast two-hybrid assays as well as in FRET experiments performed in plant cells. The interaction was abolished

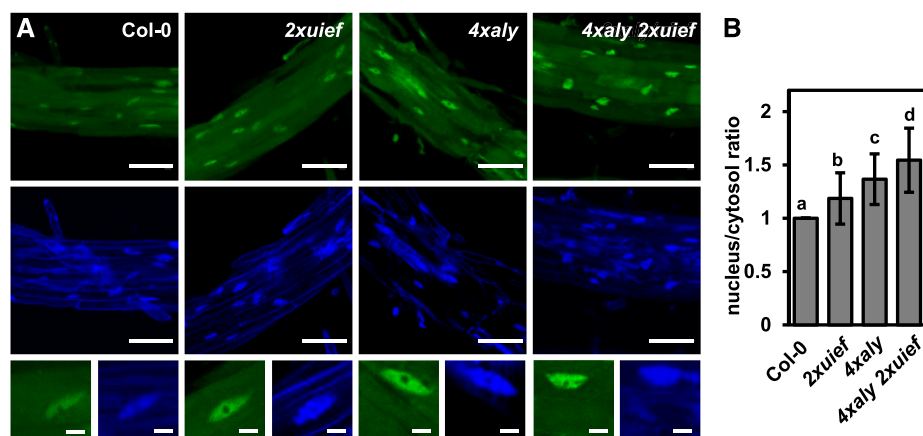


Figure 7. Analysis of nucleocytoplasmic distribution of polyadenylated mRNA. A, Root cells of 6-DAS Col-0, *2xuiief*, *4xaly*, and *4xaly 2xuiief* seedlings were examined using whole mount in situ hybridization with a fluorescently labeled 48-nt oligo(dT) probe. CLSM images (taken using identical microscope settings) of representative regions of the analyzed roots (top). Images representing the DAPI fluorescence of the same root regions (middle). Examples of individual cells with both the fluorescence signal of oligo(dT; green) and DAPI (blue) are shown (bottom). Size bars represent 60 μm (top, middle) and 10 μm (bottom). B, The fluorescent hybridization signal of nucleoplasm relative to that of the cytosol was quantified for ≥ 50 nuclei from three roots of each genotype (x axis). The ratios are depicted relative to that in Col-0 (ratio: 1). Data were analyzed by one-way analysis of variance and error bars indicate SD . The letters above the histogram bars indicate the outcome of a multicomparison Tukey's test ($P < 0.001$).

by mutating the UBM of UIEF1, indicating that the association with UAP56 is conserved between UIF and its plant orthologs. Therefore, in Arabidopsis, UIEF1/2 likely is recruited via UAP56, similar to the ALY1–4 mRNA export factors (Pfaff et al., 2018).

RNA-binding is a characteristic feature of many mRNA export factors (Walsh et al., 2010). Despite the absence of known RNA-binding motifs, in MST experiments UIEF1 binds ssRNA, albeit with only minor preference over dsRNA and ssDNA. The binding affinity of UIEF1 for ssRNA is in the same range (964 nM) as determined in comparable measurements for Arabidopsis ALY1 (481 nM; Pfaff et al., 2018). Human UIF binds ssRNA as evident from in vitro UV crosslinking experiments (Hautbergue et al., 2009). Comparing the RNA-binding of full-length and truncated versions of UIEF1 demonstrated that the C-terminal part of the protein mainly contributes to the RNA interaction. The C-terminal part of UIEF1 is rich in the amino acid residues Arg, Gln, and Gly, and it contains as its most highly conserved region a predicted α -helix (Leu-167–Met-179; compare with Supplemental Fig. S1) based on analysis using the I-TASSER server (Yang and Zhang, 2015), but it remains to be seen whether this region is critical for RNA interactions. Unlike Arabidopsis ALY1, which bound m⁵C-modified RNA with ~3-fold higher affinity than the unmodified control RNA (Pfaff et al., 2018), UIEF1 displayed only a minor preference for the m⁵C-modified probe in a comparable experiment. This suggests that preferential binding to m⁵C-modified RNA is a property of ALY proteins (Yang et al., 2017; Pfaff et al., 2018), but not of UIEF mRNA export factors.

According to public transcript profiling data (Supplemental Fig. S7), the *UIEF1* and *UIEF2* transcripts occur widely in vegetative Arabidopsis tissues including roots and leaves. Consistently, UIEF1- and UIEF2-GFP fusion proteins expressed under control of the respective native promoters are detected in all root cells. However, our experiments revealed that relative to comparable analyses with ALY-GFP fusion proteins (Pfaff et al., 2018), the fluorescence signals of UIEF1/2-GFP were considerably weaker, suggesting lower expression levels. The lower level of expression, in combination with the high natural autofluorescence and reabsorption of emitted GFP fluorescence within leaf tissue, are considered as primary reasons why we were unable to unequivocally detect UIEF1/2-GFP fluorescence in leaves. The weak expression of UIEF1/2 observed in Arabidopsis is in line with the situation in mouse cells, where UIF is expressed at ~40-fold lower protein levels than ALY (Heath et al., 2016).

In common with human UIF-GFP (Hautbergue et al., 2009), UIEF1/2-GFP fluorescence was specifically detected in Arabidopsis cell nuclei. mRNA export adaptors dissociate from the mRNP before/during translocation through the NPC (Walsh et al., 2010), and thus remain nuclear. Like the Arabidopsis ALY1–4 proteins (Pfaff et al., 2018), in addition to nucleoplasmic

localization, UIEF1/2 show accumulation in nucleoli in some cells, which may seem surprising. However, nucleoli are involved in other RNA-dependent processes in addition to rRNA/ribosome biogenesis, including mRNA splicing and export (Shaw and Brown, 2012; Meier et al., 2017). The export of preribosomal particles in yeast and metazoa occurs by mechanisms involving exportins/CRM1 (Peña et al., 2017), which apparently is conserved in plants (Merkle, 2011; Chen et al., 2012). Still, we have examined whether the accumulation of rRNAs is affected in plants lacking UIEF1/2 and/or ALY1–4. The ratio of cytosolic rRNA species relative to plastid rRNAs (that served as a reference) was unaltered in *2xuiief*, *4xaly*, and *4xaly 2xuiief* plants, indicating that, as expected, UIEF1/2 and ALY1–4 are not involved in ribosome biogenesis. Therefore, the reason for the partial nucleolar localization of UIEF1/2 and ALY1–4 proteins remains obscure.

Inactivation of the *UIEF1/2* genes caused only mild growth defects in the single- and double-mutant plants. The fact that *uief1* and *uief2* single and double mutants are phenotypically similar suggests that the UIEF1/2 proteins have redundant functions. The combination of the *2xuiief* with the *4xaly* mutations in the *4xaly 2xuiief* plants resulted in reduced plant height and rosette diameter compared to that of the parental lines. Therefore, the concurrent loss of UIEF1/2 and ALY1–4 additively influence these growth parameters, which is paralleled by an increased mRNA accumulation in the nuclei of *4xaly 2xuiief* plants. On the contrary, the *uief1* and *uief2* mutations do not influence the developmental parameters (i.e. bolting), which are clearly affected in the *4xaly* plants (Pfaff et al., 2018). Likewise, we neither observed any reproductive effect in the *2xuiief* mutant, nor additive reproductive phenotypes when *UIEF1* and *UIEF2* are lacking in the *4xaly* background. A possible explanation is the absence of UIEF1 and UIEF2 in o-vules and pollen, which is supported by the lack of detectable UIEF1-GFP and UIEF2-GFP fluorescence in these tissues (data not shown).

UIF-like proteins occur in metazoa and plants (Hautbergue et al., 2009), and depending on the species, mono- and dicot plants encode one or two UIF-like proteins. Knock-down of the human and *D. melanogaster* ALY caused a modest accumulation of bulk mRNAs in the nucleus (Gatfield and Izaurralde, 2002; Katahira et al., 2009), whereas upon depletion of ALY proteins in *C. elegans*, no mRNA export defect was detectable (Longman et al., 2003). Knock-down of human UIF did not result in nuclear accumulation of polyadenylated mRNAs, whereas simultaneous knock-down of UIF and ALY caused a clear mRNA export defect (Hautbergue et al., 2009). Similarly, Arabidopsis *uief1/2* single- and double-mutants showed a weaker nuclear accumulation of polyadenylated mRNAs than the *4xaly* mutant, and the *4xaly 2xuiief* mutant showed distinctly enhanced mRNA export defects compared with *4xaly* plants. These results indicate that both UIEF1/2 and ALY1–4 are important for efficient nucleocytoplasmic mRNA transport.

Moreover, the fact that *4xaly 2xuiief* mutant plants lacking all ALY1–4 and UIEF1/2 proteins are viable and their mRNA export block is severe, but still incomplete, suggests that, similar to the situation in metazoa (Heath et al., 2016), additional mRNA export adaptors exist. Because orthologs of human Chtop and Luzp4 (Chang et al., 2013; Viphakone et al., 2015) apparently do not exist in plants, shuttling serine/arginine-rich (SR) proteins are likely candidates (Huang et al., 2003; Müller-McNicoll et al., 2016). RNA-binding SR proteins that show a dynamic nucleocytoplasmic distribution have been also characterized from plants (Tillemans et al., 2005; Rausin et al., 2010), but currently it is unclear whether they are involved in mRNA export. The fact that loss of individual mRNA export factors causes only insignificant effects on the nucleocytoplasmic distribution of mRNAs suggests that there is functional redundancy between related factors such as ALY and UIEF (Heath et al., 2016). At the same time, it is possible that certain export factors are preferentially recruited to distinct subsets of mRNAs to mediate their nucleocytoplasmic transport.

CONCLUSION

Apart from components of the NPC (Parry, 2015; Meier et al., 2017) and the TREX-2 complex that is situated at the nucleoplasmic side of the NPC (Lu et al., 2010), only a few factors have been experimentally analyzed for their involvement in plant mRNA export. These include subunits of the THO core complex of TREX (Pan et al., 2012; Xu et al., 2015; Sørensen et al., 2017), MOS11 and ALY1–4 proteins (Germain et al., 2010; Pfaff et al., 2018). Loss of these proteins results in mRNA accumulation in the nucleus, as demonstrated by *in situ* hybridization analyses using oligo (dT) probes. Here, we provide evidence that the Arabidopsis nuclear RNA-binding proteins UIEF1 and UIEF2 that interact with the RNA helicase UAP56 are additional factors that contribute to the mRNA export in plants. In cell nuclei of *uief1/2* mutant plants, mRNAs accumulate and the *uief1/2* mutations enhance the previously observed mRNA export defect of *4xaly* plants. Similarly, *uief1/2* mutations cause modest growth deficiencies and they augment some growth defects of *4xaly* plants. These results imply that UIEF1/2 and ALY1–4 cooperate to mediate the efficient nucleocytoplasmic transport of mRNAs in plants.

MATERIALS AND METHODS

Plant Material and Documentation

Arabidopsis (*Arabidopsis thaliana*; Col-0) was grown at 21°C in a growth chamber under long-day (LD) conditions (16 h photoperiod per day) on soil (Antosz et al., 2017), whereas for some analyses plants were grown on Murashige & Skoog (MS) medium (Murashige and Skoog, 1962) under sterile conditions. After sowing, seeds were stratified in darkness for 48 h at 4°C before incubation in the plant growth chamber. For root analyses, plants were grown on vertically oriented MS plates in a plant incubator (Percival Scientific) under

LD conditions as described in Dürr et al. (2014). Seeds of the *uief1/2* T-DNA insertion lines were obtained from the European Arabidopsis Stock Center (<http://www.arabidopsis.info/>) and the *aly1–4* mutant lines were reported in Pfaff et al. (2018). Mutant plants were characterized by PCR-based genotyping in combination with sequencing of the insertion region and by RT-PCR (Antosz et al., 2017). By crossing the parental lines as described in Lolas et al. (2010), higher-order mutant lines were generated. Using plasmids harboring UIEF1/2-GFP fusion constructs under control of the respective native promoters (Supplemental Table S1) and *Agrobacterium*-mediated floral dip transformation as described in Pedersen et al. (2010) and Antosch et al. (2015), plants were generated that express UIEF1/2-GFP. Plant phenotypes were documented and quantified after different periods (days after stratification, DAS) as described in Dürr et al. (2014) and Antosz et al. (2017). All phenotypic analyses were independently performed at least twice and representative examples of the reproduced experiments are shown.

Plasmid Constructions

The required gene or cDNA sequences were amplified by PCR with KAPA DNA polymerase (PeqLab) using Arabidopsis genomic DNA or cDNA as template and the primers (providing also the required restriction enzyme cleavage sites) listed in Supplemental Table S1. The PCR fragments were inserted into suitable plasmids using standard methods. All plasmid constructions were checked by DNA sequencing, and details of the plasmids generated in this work are summarized in Supplemental Table S1.

Yeast Two-Hybrid Assays

Yeast two-hybrid assays were essentially performed according to the manufacturer (Clontech). In brief, yeast cells of the strain AH109 were cotransformed with pGBKT7 and pGADT7 plasmids (Supplemental Table S1) and grown at 30°C on SD/-Leu/-Trp (DDO) medium. For interaction assays, cells were grown on SD/-Ade/-Leu/-Trp/-His (QDO) medium for 2 d (Kammel et al., 2013). As positive and negative controls served the interactions between p53 and the SV40 large T-antigen, and between lamin and the SV40 large T-antigen, respectively, provided by the manufacturer.

FRET

FRET-APB was essentially performed as described in Weidtkamp-Peters and Stahl (2017) using an SP8 microscope (Leica). Briefly, a square (0.5 × 0.5 cm) of an infiltrated *Nicotiana benthamiana* leaf was mounted in H₂O on an objective slide with the abaxial side facing up. A circular region of interest was bleached at 100% laser power, for 80 iterations. Fifteen prebleach and 15 postbleach images were analyzed using the software LAS X (Leica). The mean FRET efficiency was calculated as follows: $(I_{POST} - I_{PRE}) / I_{PRE} \times 100$, with I_{POST} = mean fluorescence intensity of 15 postbleached frames and I_{PRE} = mean fluorescence intensity of 15 prebleached frames.

Production of Recombinant Proteins

Full-length UIEF1 and truncated versions of the protein (Supplemental Table S1) were expressed in *E. coli* using plasmid pET24b-GB1 (Hautbergue et al., 2008) driving the expression of the UIEF1 proteins fused to a 6xHis-tag for metal-chelate purification and a GB1-tag increasing protein stability/solubility (Gronenborn et al., 1991). The proteins were isolated from *Escherichia coli* lysates by metal-chelate affinity chromatography using Ni-NTA beads (Qiagen), followed by fast protein liquid chromatography ion-exchange chromatography using a Resource Q column (GE Healthcare) as described in Pfaff et al. (2018). Finally, proteins were characterized by SDS-PAGE in combination with Coomassie staining and by mass spectrometry.

Fluorescent MST Binding Assay

MST binding experiments were carried out essentially as described in Kammel et al. (2013) with 200 nM 25-nt Cy3-labeled ssRNA, dsRNA, or ssDNA oligonucleotides or 19-nt Cy3-labeled ssRNA with or without m⁵C-modification (Yang et al., 2017; Eurofins Genomics, Supplemental Table S1). MST measurements were performed in protein buffer with a range of protein concentrations at 40% MST power, 50% light-emitting diode power in standard capillaries at 25°C on a Monolith NT.115 device (NanoTemper Technologies).

The data were analyzed using the MO Affinity Analysis software (Ver. 2.3, NanoTemper Technologies) and binding reactions were determined by analyzing changes in Temperature-Related Intensity Changes (TRIC-effect). UIEF1 data were quantified and fitted using the Hill model, as the binding curves revealed cooperative effects. To calculate the fraction bound, the ΔF_{norm} value of each point is divided by the amplitude of the fitted curve, resulting in values from 0 to 1 (0 = unbound, 1 = bound), and processed using the software KaleidaGraph 4.5 (Synergy Software).

PCR-Based Genotyping and RT-PCR

For genotyping, genomic DNA isolated from leaves was used for PCR analysis with *Taq* DNA polymerase (PeqLab) and primers specific for T-DNA insertions and the target genes (Supplemental Table S1). For RT-PCR, total RNA was extracted from ~100 mg of frozen plant tissue using the TRIzol method (Invitrogen), before the RNA samples were treated with DNase. Reverse transcription was performed using 2 μg of RNA and Revert Aid H minus M-MuLV reverse transcriptase (Thermo Fisher Scientific). The obtained cDNA was amplified by PCR using *Taq* DNA polymerase (PeqLab) as described in Dürr et al. (2014).

Analysis of Ovule Phenotypes and Seed Set

Unpollinated pistils at floral stage 12 (stage according to Smyth et al., 1990) were used to dissect and mount ovules in chloral hydrate/glycerol/water (8:1:2, w/v/v) for differential interference contrast microscopy as described in Sprunck et al. (2012). Seed set of self-pollinated siliques was investigated and photographed after overnight clearing of siliques 10–12 d after anthesis in 9:1 (v/v) ethanol/acetic acid, followed by the incubation in 90% (v/v) ethanol.

In Vitro Pollen Germination

Pollen germination experiments were carried out on solidified pollen germination medium as described in Vogler et al. (2014). Only freshly dehiscent anthers were used to release pollen grains on the germination medium. Pollinated plates were kept inside a damp box at 20°C in light for 3–5 h before microscopy and imaging.

Light Microscopy

For analysis of GFP fusion protein expression, plants of at least three independent transgenic lines each harboring the different UIEF1/2-GFP fusion constructs in the respective mutant background were selected for further analysis based on RT-PCR analysis for uniform expression of *UIEF1/2* levels similar to that in Col-0 (Antosch et al., 2015). Imaging of GFP fluorescence was performed on an inverted SP8 CLSM with a $40\times/1.3$ NA and a $63\times/1.3$ NA oil immersion objective; Leica). GFP was excited using the 488-nm argon laser line, and emission was detected from 495 to 545 nm (roots, leaves) or 500–535 nm (ovules, pollen) by a hybrid detector. Propidium iodide staining was performed as described in Dürr et al. (2014). Flowers and cleared siliques were imaged using a stereomicroscope SteREO Discovery (Ver. 8, Zeiss). Cleared ovules and 4',6-diamidino-2-phenylindole (DAPI)-stained pollen grains were investigated at the APOTOME FL (Zeiss) with a differential interference contrast objective $40\times/1.4$ oil and a 49DAPI reflector for DAPI fluorescence. Germinated pollen tubes were analyzed using an inverse Eclipse 2000-S microscope (Nikon) equipped with an Axio-Cam MRm charge-coupled device camera using a 209/0.4 NA air objective (Zeiss).

rRNA Analysis

rRNAs of total RNA preparations isolated from the aerial part of 10-d-old seedlings were analyzed and quantified using a Bioanalyser (Agilent), the RNA 6000 Nano kit (Agilent) and the software provided by the supplier. rRNA ratios were determined as described in Walter et al. (2010).

Whole Mount In Situ Hybridization

To determine the relative distribution of bulk mRNA in nuclei and cytosol, a previously described protocol was adopted (Gong et al., 2005) using 6-d-old seedlings grown on solid MS medium. Hybridization was performed in

PerfectHyb Plus solution (Sigma-Aldrich) with an Alexa Fluor 488-labeled 48-nt oligo(dT) probe. Fluorescent signals of seedling roots were analyzed using CLSM with an SP8 microscope (Leica) and quantified as described in Sørensen et al. (2017).

Accession Numbers

Sequence data for the genes described in this article can be found in the Arabidopsis Genome Initiative or GenBank/European Molecular Biology Laboratory databases under the following accession numbers: *UIEF1* (At4g10970), *UIEF2* (At4g23910), *ALY1* (At5g59950), *ALY2* (At5g02530), *ALY3* (At1g66260), *ALY4* (At5g37720), *UAP56A* (At5g11170), *UAP56B* (At5g11200).

Supplemental Data

The following supplemental materials are available.

Supplemental Figure S1. Alignment of UIF-like amino acid sequences of different mono- and dicot plants.

Supplemental Figure S2. Sequence similarity of UIF-like sequences.

Supplemental Figure S3. MST analysis of the interaction of UIEF1 and the unfused 6xHis-GB1 with nucleic acids.

Supplemental Figure S4. Molecular characterization of *uief1/2* T-DNA insertion mutants.

Supplemental Figure S5. *UIEF1/2* transcript levels of *uief1/2* mutant plants harboring UIEF1/2-GFP fusion constructs.

Supplemental Figure S6. Comparative CLSM analysis of UIEF1/2-GFP and ALY1/2-GFP.

Supplemental Figure S7. Comparison of public transcript profiling data regarding *UIEF1/2* and *ALY1–4* genes.

Supplemental Figure S8. Phenotypic characterization of *uief1/2* single- and *2xuief* double mutant plants relative to Col-0.

Supplemental Figure S9. Analysis of nucleocytoplasmic distribution of polyadenylated mRNA in *uief1/2* mutants.

Supplemental Figure S10. Phenotypic characterization of *2xuief*, *4xaly*, and *4xaly 2xuief* mutant plants relative to Col-0.

Supplemental Figure S11. *4xaly* and *4xaly 2xuief* mutants show similar reproductive defects.

Supplemental Figure S12. Accumulation of cytosolic and plastid rRNA species.

Supplemental Table S1. Oligonucleotide primers used in this study and construction of plasmids.

ACKNOWLEDGMENTS

We thank Astrid Bruckmann and Eduard Hochmuth for mass spectrometry analyses, Antje Böttinger for technical assistance, Ralph Bock for advice regarding rRNA quantification, Stuart Wilson for providing plasmid pET24b-GB1, and the Nottingham Arabidopsis Stock Centre for providing *Arabidopsis* T-DNA insertion lines.

Received November 27, 2018; accepted January 18, 2019; published January 30, 2019.

LITERATURE CITED

- Antosch M, Schubert V, Holzinger P, Houben A, Grasser KD (2015) Mitotic lifecycle of chromosomal 3xHMG-box proteins and the role of their N-terminal domain in the association with rDNA loci and proteolysis. *New Phytol* **208**: 1067–1077
- Antosch W, Pfab A, Ehrnsberger HF, Holzinger P, Köllen K, Mortensen SA, Bruckmann A, Schubert T, Längst G, Griesenbeck J, et al (2017) The composition of the *Arabidopsis* RNA polymerase II transcript

- elongation complex reveals the interplay between elongation and mRNA processing factors. *Plant Cell* **29**: 854–870
- Chang CT, Hautbergue GM, Walsh MJ, Viphakone N, van Dijk TB, Philipsen S, Wilson SA** (2013) Chtop is a component of the dynamic TREX mRNA export complex. *EMBO J* **32**: 473–486
- Chen MQ, Zhang AH, Zhang Q, Zhang BC, Nan J, Li X, Liu N, Qu H, Lu CM, Sudmorgen, et al** (2012) *Arabidopsis* NMD3 is required for nuclear export of 60S ribosomal subunits and affects secondary cell wall thickening. *PLoS One* **7**: e35904
- Dufu K, Livingstone MJ, Seebacher J, Gygi SP, Wilson SA, Reed R** (2010) ATP is required for interactions between UAP56 and two conserved mRNA export proteins, Aly and CIP29, to assemble the TREX complex. *Genes Dev* **24**: 2043–2053
- Dürr J, Lolas IB, Sørensen BB, Schubert V, Houben A, Melzer M, Deutzmann R, Grasser M, Grasser KD** (2014) The transcript elongation factor SPT4/SPT5 is involved in auxin-related gene expression in *Arabidopsis*. *Nucleic Acids Res* **42**: 4332–4347
- Fleischmann TT, Scharff LB, Alkatib S, Hasdorf S, Schöttler MA, Bock R** (2011) Nonessential plastid-encoded ribosomal proteins in tobacco: A developmental role for plastid translation and implications for reductive genome evolution. *Plant Cell* **23**: 3137–3155
- Gaouar O, Germain H** (2013) mRNA export: Threading the needle. *Front Plant Sci* **4**: 59
- Gatfield D, Izaurralde E** (2002) REF1/Aly and the additional exon junction complex proteins are dispensable for nuclear mRNA export. *J Cell Biol* **159**: 579–588
- Germain H, Qu N, Cheng YT, Lee E, Huang Y, Dong OX, Gannon P, Huang S, Ding P, Li Y, et al** (2010) MOS11: A new component in the mRNA export pathway. *PLoS Genet* **6**: e1001250
- Gong Z, Dong CH, Lee H, Zhu J, Xiong L, Gong D, Stevenson B, Zhu JK** (2005) A DEAD box RNA helicase is essential for mRNA export and important for development and stress responses in *Arabidopsis*. *Plant Cell* **17**: 256–267
- Gronenborn AM, Filpula DR, Essig NZ, Achari A, Whitlow M, Wingfield PT, Clore GM** (1991) A novel, highly stable fold of the immunoglobulin binding domain of streptococcal protein G. *Science* **253**: 657–661
- Hautbergue GM, Hung ML, Golovanov AP, Lian LY, Wilson SA** (2008) Mutually exclusive interactions drive handover of mRNA from export adaptors to TAP. *Proc Natl Acad Sci USA* **105**: 5154–5159
- Hautbergue GM, Hung ML, Walsh MJ, Snijders AP, Chang CT, Jones R, Ponting CP, Dickman MJ, Wilson SA** (2009) UIF, a New mRNA export adaptor that works together with REF/ALY, requires FACT for recruitment to mRNA. *Curr Biol* **19**: 1918–1924
- Heath CG, Viphakone N, Wilson SA** (2016) The role of TREX in gene expression and disease. *Biochem J* **473**: 2911–2935
- Huang Y, Gattoni R, Stévenin J, Steitz JA** (2003) SR splicing factors serve as adapter proteins for TAP-dependent mRNA export. *Mol Cell* **11**: 837–843
- Kammel C, Thomaier M, Sørensen BB, Schubert T, Längst G, Grasser M, Grasser KD** (2013) *Arabidopsis* DEAD-box RNA helicase UAP56 interacts with both RNA and DNA as well as with mRNA export factors. *PLoS One* **8**: e60644
- Katahira J** (2012) mRNA export and the TREX complex. *Biochim Biophys Acta* **1819**: 507–513
- Katahira J, Inoue H, Hurt E, Yoneda Y** (2009) Adaptor Aly and co-adaptor Thoc5 function in the Tap-p15-mediated nuclear export of HSP70 mRNA. *EMBO J* **28**: 556–567
- Köhler A, Hurt E** (2007) Exporting RNA from the nucleus to the cytoplasm. *Nat Rev Mol Cell Biol* **8**: 761–773
- Lolas IB, Himanen K, Grönlund JT, Lynggaard C, Houben A, Melzer M, Van Lijsebettens M, Grasser KD** (2010) The transcript elongation factor FACT affects *Arabidopsis* vegetative and reproductive development and genetically interacts with *HUB1/2*. *Plant J* **61**: 686–697
- Longman D, Johnstone IL, Cáceres JF** (2003) The Ref/Aly proteins are dispensable for mRNA export and development in *Caenorhabditis elegans*. *RNA* **9**: 881–891
- Lu Q, Tang X, Tian G, Wang F, Liu K, Nguyen V, Kohalmi SE, Keller WA, Tsang EW, Harada JJ, et al** (2010) *Arabidopsis* homolog of the yeast TREX-2 mRNA export complex: Components and anchoring nucleoporin. *Plant J* **61**: 259–270
- Luo ML, Zhou Z, Magni K, Christoforides C, Rappsilber J, Mann M, Reed R** (2001) Pre-mRNA splicing and mRNA export linked by direct interactions between UAP56 and Aly. *Nature* **413**: 644–647
- Masuda S, Das R, Cheng H, Hurt E, Dorman N, Reed R** (2005) Recruitment of the human TREX complex to mRNA during splicing. *Genes Dev* **19**: 1512–1517
- Meier I, Richards EJ, Evans DE** (2017) Cell biology of the plant nucleus. *Annu Rev Plant Biol* **68**: 139–172
- Merkle T** (2011) Nucleo-cytoplasmic transport of proteins and RNA in plants. *Plant Cell Rep* **30**: 153–176
- Müller-McNicoll M, Botti V, de Jesus Domingues AM, Brandl H, Schwich OD, Steiner MC, Curk T, Poser I, Zarnack K, Neugebauer KM** (2016) SR proteins are NXF1 adaptors that link alternative RNA processing to mRNA export. *Genes Dev* **30**: 553–566
- Murashige T, Skoog F** (1962) A revised medium for rapid growth and bioassay with tobacco tissue cultures. *Physiol Plant* **15**: 473–497
- Pan H, Liu S, Tang D** (2012) HPR1, a component of the THO/TREX complex, plays an important role in disease resistance and senescence in *Arabidopsis*. *Plant J* **69**: 831–843
- Parry G** (2015) The plant nuclear envelope and regulation of gene expression. *J Exp Bot* **66**: 1673–1685
- Pedersen DS, Merkle T, Markt B, Lildballe DL, Antosch M, Bergmann T, Tönsing K, Anselmetti D, Grasser KD** (2010) Nucleocytoplasmic distribution of the *Arabidopsis* chromatin-associated HMGB2/3 and HMGB4 proteins. *Plant Physiol* **154**: 1831–1841
- Peña C, Hurt E, Panse VG** (2017) Eukaryotic ribosome assembly, transport and quality control. *Nat Struct Mol Biol* **24**: 689–699
- Pfaff C, Ehrnsberger HF, Flores-Tornero M, Sørensen BB, Schubert T, Längst G, Griesenbeck J, Sprunck S, Grasser M, Grasser KD** (2018) ALY RNA-binding proteins are required for nucleocytoplasmic mRNA transport and modulate plant growth and development. *Plant Physiol* **177**: 226–240
- Rausin G, Tillemans V, Stankovic N, Hanikenne M, Motte P** (2010) Dynamic nucleocytoplasmic shuttling of an *Arabidopsis* SR splicing factor: Role of the RNA-binding domains. *Plant Physiol* **153**: 273–284
- Shaw P, Brown J** (2012) Nucleoli: Composition, function, and dynamics. *Plant Physiol* **158**: 44–51
- Smyth DR, Bowman JL, Meyerowitz EM** (1990) Early flower development in *Arabidopsis*. *Plant Cell* **2**: 755–767
- Sørensen BB, Ehrnsberger HF, Esposito S, Pfaff A, Bruckmann A, Hauptmann J, Meister G, Merkl R, Schubert T, Längst G, et al** (2017) The *Arabidopsis* THO/TREX component TEX1 functionally interacts with MOS11 and modulates mRNA export and alternative splicing events. *Plant Mol Biol* **93**: 283–298
- Sprunck S, Rademacher S, Vogler F, Gheyselinck J, Grossniklaus U, Dresselhaus T** (2012) Egg cell-secreted EC1 triggers sperm cell activation during double fertilization. *Science* **338**: 1093–1097
- Strässer K, Hurt E** (2000) Yra1p, a conserved nuclear RNA-binding protein, interacts directly with Mex67p and is required for mRNA export. *EMBO J* **19**: 410–420
- Strässer K, Masuda S, Mason P, Pfannstiel J, Oppizzi M, Rodríguez-Navarro S, Rondón AG, Aguilera A, Struhl K, Reed R, et al** (2002) TREX is a conserved complex coupling transcription with messenger RNA export. *Nature* **417**: 304–308
- Taniguchi I, Ohno M** (2008) ATP-dependent recruitment of export factor Aly/REF onto intronless mRNAs by RNA helicase UAP56. *Mol Cell Biol* **28**: 601–608
- Tillemans V, Dispa L, Remacle C, Collinge M, Motte P** (2005) Functional distribution and dynamics of *Arabidopsis* SR splicing factors in living plant cells. *Plant J* **41**: 567–582
- Viphakone N, Hautbergue GM, Walsh M, Chang CT, Holland A, Folco EG, Reed R, Wilson SA** (2012) TREX exposes the RNA-binding domain of Nxf1 to enable mRNA export. *Nat Commun* **3**: 1006
- Viphakone N, Cumberbatch MG, Livingstone MJ, Heath PR, Dickman MJ, Catto JW, Wilson SA** (2015) Luzp4 defines a new mRNA export pathway in cancer cells. *Nucleic Acids Res* **43**: 2353–2366
- Vogler F, Schmalzl C, Enghart M, Bircheneder M, Sprunck S** (2014) Brassinosteroids promote *Arabidopsis* pollen germination and growth. *Plant Reprod* **27**: 153–167
- Walsh MJ, Hautbergue GM, Wilson SA** (2010) Structure and function of mRNA export adaptors. *Biochem Soc Trans* **38**: 232–236
- Walter M, Piepenburg K, Schöttler MA, Petersen K, Kahlau S, Tiller N, Drechsel O, Weingartner M, Kudla J, Bock R** (2010) Knockout of the plastid RNase E leads to defective RNA processing and chloroplast ribosome deficiency. *Plant J* **64**: 851–863

- Weidtkamp-Peters S, Stahl Y** (2017) The use of FRET/FLIM to study proteins interacting with plant receptor kinases. *Methods Mol Biol* **1621**: 163–175
- Wickramasinghe VO, Laskey RA** (2015) Control of mammalian gene expression by selective mRNA export. *Nat Rev Mol Cell Biol* **16**: 431–442
- Williams T, Ngo LH, Wickramasinghe VO** (2018) Nuclear export of RNA: Different sizes, shapes and functions. *Semin Cell Dev Biol* **75**: 70–77
- Xu XM, Meier I** (2008) The nuclear pore comes to the fore. *Trends Plant Sci* **13**: 20–27
- Xu C, Zhou X, Wen CK** (2015) HYPER RECOMBINATION1 of the THO/TREX complex plays a role in controlling transcription of the *REVERSION-TO-ETHYLENE SENSITIVITY1* gene in *Arabidopsis*. *PLoS Genet* **11**: e1004956
- Yang J, Zhang Y** (2015) I-TASSER server: New development for protein structure and function predictions. *Nucleic Acids Res* **43**(W1): W174–W81
- Yang X, Yang Y, Sun BF, Chen YS, Xu JW, Lai WY, Li A, Wang X, Bhattarai DP, Xiao W, et al** (2017) 5-methylcytosine promotes mRNA export—NSUN2 as the methyltransferase and ALYREF as an m⁵C reader. *Cell Res* **27**: 606–625
- Yelina NE, Smith LM, Jones AME, Patel K, Kelly KA, Baulcombe DC** (2010) Putative *Arabidopsis* THO/TREX mRNA export complex is involved in transgene and endogenous siRNA biosynthesis. *Proc Natl Acad Sci USA* **107**: 13948–13953
- Zenkhusen D, Vinciguerra P, Strahm Y, Stutz F** (2001) The yeast hnRNP-Like proteins Yra1p and Yra2p participate in mRNA export through interaction with Mex67p. *Mol Cell Biol* **21**: 4219–4232